Author/s:
Giuffrida, L;Sek, K;Henderson, MA;House, IG;Lai, J;Chen, AXY;Todd, KL;Petley, EV;Mardiana, S;Todorovski, I;Gruber, E;Kelly, MJ;Solomon, BJ;Vervoort, SJ;Johnstone, RW;Parish, IA;Neeson, PJ;Kats, LM;Darcy, PK;Beavis, PA

Title:
IL-15 Preconditioning Augments CAR T Cell Responses to Checkpoint Blockade for Improved Treatment of Solid Tumors

Date:
2020-11-04

Citation:
Giuffrida, L., Sek, K., Henderson, M. A., House, I. G., Lai, J., Chen, A. X. Y., Todd, K. L., Petley, E. V., Mardiana, S., Todorovski, I., Gruber, E., Kelly, M. J., Solomon, B. J., Vervoort, S. J., Johnstone, R. W., Parish, I. A., Neeson, P. J., Kats, L. M., Darcy, P. K. & Beavis, P. A. (2020). IL-15 Preconditioning Augments CAR T Cell Responses to Checkpoint Blockade for Improved Treatment of Solid Tumors. Molecular Therapy, 28 (11), pp.2379-2393. https://doi.org/10.1016/j.ymthe.2020.07.018.

Persistent Link:
https://hdl.handle.net/11343/331896

Molecular Therapy
Original Article

IL-15 Preconditioning Augments CAR T Cell Responses to Checkpoint Blockade for Improved Treatment of Solid Tumors

Lauren Giuffrida,[1,2] Kevin Sek,[1,2] Melissa A. Henderson,[1,2] Imran G. House,[1,2] Junyun Lai,[1,2] Amanda X.Y. Chen,[1,2] Kirsten L. Todd,[1,2] Emma V. Petley,[1,2] Sherly Mardiana,[1,2] Izabela Todorovski,[2,3] Emily Gruber,[2,3] Madison J. Kelly,[2,3] Benjamin J. Solomon,[2] Stephin J. Vervoort,[2,3] Ricky W. Johnstone,[2,3] Ian A. Parish,[1,2] Paul J. Neeson,[1,2] Lev M. Kats,[2,3] Phillip K. Darcy,[1,2,4,5,6] and Paul A. Beavis[1,2,6]

[1]Cancer Immunology Program, Peter MacCallum Cancer Centre, Melbourne, VIC 3000, Australia; [2]Sir Peter MacCallum Department of Oncology, The University of Melbourne, Parkville, VIC 3010, Australia; [3]Translational Haematology Program, Peter MacCallum Cancer Centre, Melbourne, VIC 3000, Australia; [4]Department of Pathology, The University of Melbourne, Parkville, VIC 3010, Australia; [5]Department of Immunology, Monash University, Clayton, VIC 3168, Australia

Chimeric antigen receptor (CAR) T cell therapy has been highly successful in hematological malignancies leading to their US Food and Drug Administration (FDA) approval. However, the efficacy of CAR T cells in solid tumors is limited by tumor-induced immunosuppression, leading to the development of combination approaches, such as adjuvant programmed cell death 1 (PD-1) blockade. Current FDA-approved methods for generating CAR T cells utilize either anti-CD3 and interleukin (IL)-2 or anti-CD3/CD28 beads, which can generate a T cell product with an effector/exhausted phenotype. Whereas different cytokine preconditioning milieu, such as IL-7/IL-15, have been shown to promote T cell engraftment, the impact of this approach on CAR T cell responses to adjuvant immune-checkpoint blockade has not been assessed. In the current study, we reveal that the preconditioning of CAR T cells with IL-7/IL-15 increased CAR T cell responses to anti-PD-1 adjuvant therapy. This was associated with the emergence of an intratumoral $CD8^+CD62L^+TCF7^+IRF4^-$ population that was highly responsive to anti-PD-1 therapy and mediated the vast majority of transcriptional and epigenetic changes *in vivo* following PD-1 blockade. Our data indicate that preservation of CAR T cells in a $TCF7^+$ phenotype is crucial for their responsiveness to adjuvant immunotherapy approaches and should be a key consideration when designing clinical protocols.

INTRODUCTION

Immunotherapy of cancer with immune-checkpoint inhibitors, such as anti-programmed cell death 1 (PD-1), is now an established paradigm, particularly for the treatment of patients with high numbers of lymphocytes infiltrating their tumors. For patients with immunologically "cold" tumors, one treatment option is the use of chimeric antigen receptor (CAR) T cells. The generation of CAR T cells involves the *ex vivo* transduction of a patient's T cells with a CAR that is designed to recognize a specified tumor antigen through a single-chain variable fragment (scFv), while providing intracellular signaling domains, such as CD3ζ, CD28, and/or 4-1BB. These intracellular signaling domains allow for robust T cell activation and expansion following antigen stimulation.[1–4] CAR T cells have been successful in the treatment of hematological malignancies, such as acute lymphoblastic leukemia and diffuse large B cell lymphoma, leading to their recent US Food and Drug Administration (FDA) approval. The success of CAR T cells in solid tumors, however, has been limited to date. The reasons for the failure of CAR T cells in solid tumors are currently under investigation, but factors of importance include the immunosuppressive microenvironment, suboptimal trafficking of T cells to the tumor site, and a failure of the CAR T cells to engraft and expand *in vivo*, as is observed with CD19-targeting CAR T cells.[5,6]

The adoptive transfer of central memory (CM) or stem cell memory (SCM) T (T_{CM} and T_{SCM}, respectively) cells results in enhanced therapeutic activity due to their increased long-term persistence.[7,8] Modulation of T cell differentiation by manipulation of the cytokine milieu[9,10] or the use of epigenetic modifiers[11,12] to preserve the T_{CM} phenotype prior to treatment are promising strategies to enhance the effectiveness of CAR T cell therapy. However, although enhancing the persistence of CAR T cells can enhance their therapeutic activity in hematological malignancies, this does not address the significant barrier of local tumor immunosuppression, which limits the effectiveness of CAR T cells in solid tumors. The use of checkpoint inhibitors, such as anti-PD-1 or CRISPR-mediated deletion of PD-1, can

Received 28 April 2020; accepted 10 July 2020;
https://doi.org/10.1016/j.ymthe.2020.07.018.

[6]These authors contributed equally to this work.

Correspondence: Paul A. Beavis, Cancer Immunology Program, Peter MacCallum Cancer Centre, Melbourne, VIC 3000, Australia.
E-mail: paul.beavis@petermac.org
Correspondence: Phillip K. Darcy, Cancer Immunology Program, Peter MacCallum Cancer Centre, Melbourne, VIC 3000, Australia.
E-mail: phil.darcy@petermac.org

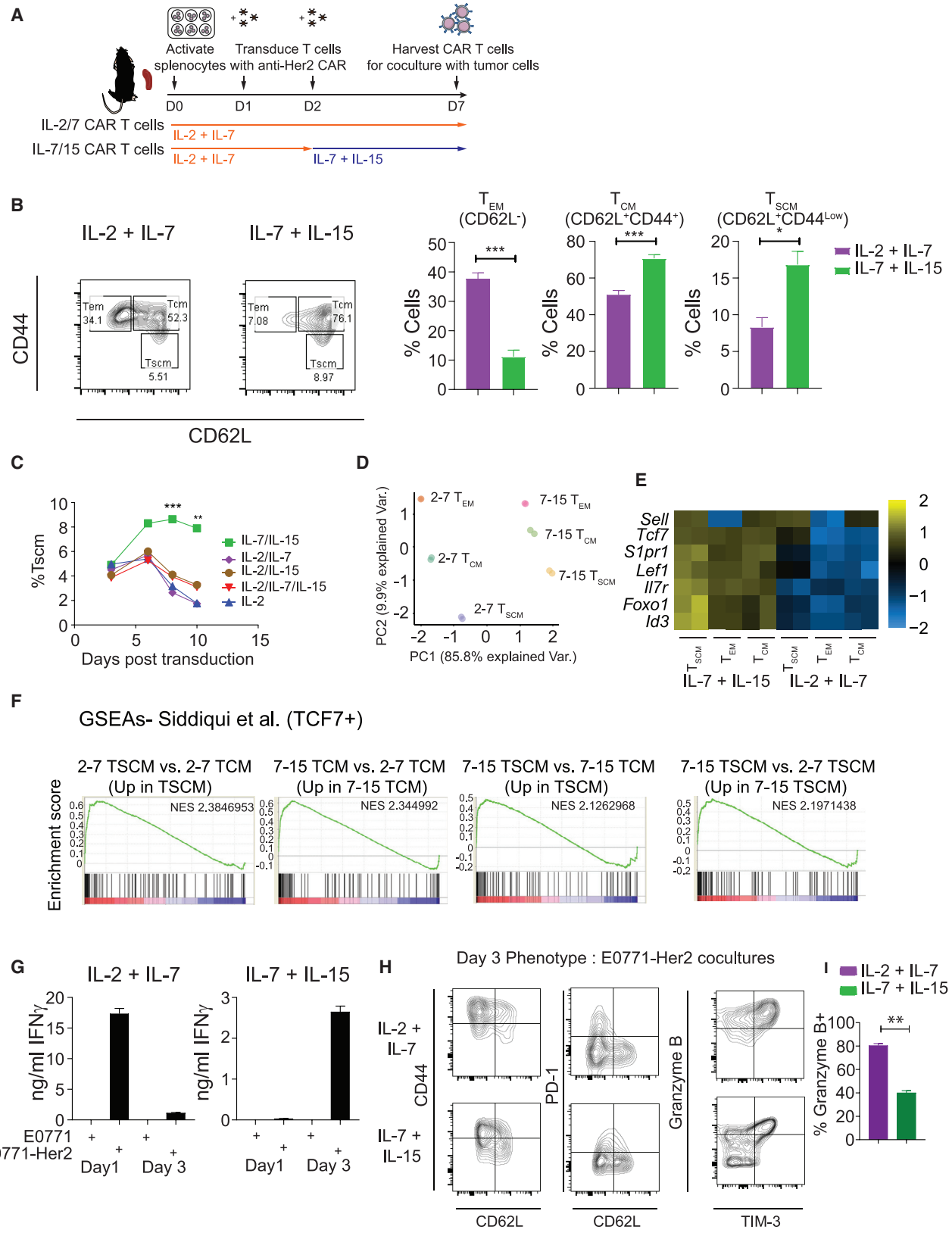

(legend on next page)

enhance CAR T cell function through prevention of interactions with inhibitory ligands, e.g., programmed death-ligand (PD-L)1/PD-L2, leading to enhanced T cell proliferation and production of proinflammatory cytokines.[13–16] PD-1 targeting, in combination with CAR T cells, has shown promise in the clinic,[17,18] and several other trials evaluating this approach are ongoing (ClinicalTrials.gov: NCT03287817, NCT02926833, and NCT02706405). Given the exciting promise of this combination, it is important to generate a CAR T cell product with the greatest potential to respond to anti-PD-1 therapy. Recent data in patients treated with checkpoint inhibitors (in the absence of adoptive T cell therapy) indicate that response rates correlate with higher levels of "progenitor exhausted" cells that express transcription factor 7 (*TCF7*; encodes the protein also known as TCF1, herein referred to as TCF7).[19,20] We therefore hypothesized that the preconditioning of CAR T cells to maintain this phenotype may maximize the effects of anti-PD-1 adjuvant therapy. This is of imperative clinical importance because current FDA-approved methods for generating CAR T cells utilize either anti-CD3 and interleukin (IL)-2 or anti-CD3/CD28 beads that can generate an effector/exhausted T cell product. Moreover, ongoing trials testing the combination of CAR T cells and anti-PD-1/PD-L1 utilize these standard stimulation protocols, which may generate a CAR T cell product with limited potential to respond to PD-1 blockade.[5,6] To investigate this, we chose to investigate the utility of IL-15 in this context, given it is a cytokine that has previously been shown to favor T_{CM} formation[10] and is used in some emerging CAR T cell clinical trial protocols (ClinicalTrials.gov: NCT03721068 and NCT02992834). Our studies revealed that IL-7/IL-15 preconditioning promoted both the quantity and quality of T_{CM} cells relative to standard preconditioning in IL-2/IL-7. Thus, IL-15 increased both the proportion of T cells exhibiting a CD62 ligand $(CD62L)^+CD44^+$ T_{CM} phenotype, enhanced their expression of memory-associated genes, including *TCF7*, and exhibited a favorable epigenetic state relative to T_{CM} cells cultured in IL-2. *In vivo*, CAR T cells generated with IL-7/IL-15 displayed increased persistence and responsiveness to anti-PD-1 treatment; CAR T cells generated in this manner exhibited increased numbers at the tumor site and produced higher levels of interferon (IFN)-γ and tumor necrosis factor (TNF) following anti-PD-1 treatment. The $CD62L^+TCF7^+$ population was highly responsive to PD-1 blockade and accounted for the majority of transcriptional and epigenetic changes evoked following anti-PD-1 therapy. Our study therefore highlights that cytokine preconditioning can significantly modulate CAR T cell responses to adjuvant immunotherapies and enhance overall therapeutic efficacy in solid tumors. These findings indicate that modulation of the cytokine milieu is an effective and rapidly translatable way to increase the combinatorial benefit of CAR T cell therapy and immune-checkpoint blockade in solid tumors. This is of high importance since current ongoing trials utilizing a combination of CAR T cells and anti-PD-1 have not attempted to preserve the $TCF7^+$ population of CAR T cells prior to treatment in order to achieve optimal synergistic effects.

RESULTS

Generation of CAR T Cells in IL-7/IL-15 Maintains T_{CM} and T_{SCM} Cells with a $TCF7^{high}$ Phenotype

In our previous studies, we have generated anti-Her2 CAR T cells via activation and transduction with anti-CD3/anti-CD28, followed by culture in a cytokine milieu of IL-2 and IL-7 (IL-2/IL-7 CAR T cells). At day 7 post-activation, this preconditioning resulted in a CAR T cell population with an approximate 4:1 ratio of $CD8^+$ to $CD4^+$ and a mixture of $CD62L^+CD44^+$ T_{CM} and $CD62L^-CD44^+$ effector memory T (T_{EM}) cells at a ratio of approximately 1:1 within the $CD8^+$ T cell subset. In order to develop a system to assess CAR T cells in a less differentiated state, we alternatively generated CAR T cells with IL-7 and IL-15 (Figure 1A). Culturing in IL-7/IL-15 (herein referred to as IL-7/IL-15 CAR T cells) resulted in a significant increase in $CD62L^+CD44^+$ T_{CM} cells within the $CD8^+$ T cell subset (Figure 1B) but did not affect the proportion of $CD4^+$ T cells expressing CD62L or CD44 and had only a minor impact on the CD8:CD4 ratio (Figures S1A and S1B). Interestingly, culturing of CAR T cells in IL-7/IL-15 did not affect the transduction efficiency, as shown by the percentage of $CD8^+$ T cells expressing the marker gene nerve growth factor receptor (NGFR) but did significantly reduce the expression of the CAR at day 6 post-activation, as shown by binding of a myc tag-directed monoclonal antibody, which binds a tag epitope within the CAR (Figures S1C and S1D). Notably, however, restimulation of IL-7/IL-15 CAR T cells with anti-CD3/anti-CD28 enhanced CAR expression in line with levels observed in IL-2/IL-7 CAR T cells, indicating that they retained potential to express high levels of the CAR (Figure S1E). A closer analysis of the memory phenotype of the $CD8^+$ subset revealed that IL-7 and IL-15 treatment led to an increased proportion of $CD62L^+CD44^{dim}$ cells, which have previously been reported to exhibit stem cell-like properties,[21] which we refer to herein as T_{SCM} (Figure 1B). A time course analysis revealed that

Figure 1. Preconditioning Anti-Her2 CAR T Cells with IL-7/IL-15 Leads to Increased Expression of Memory-Associated Genes

Anti-Her2 CAR T cells were generated in IL-2 (100 U/mL) and IL-7 (200 pg/mL) or IL-7 and IL-15 (10 ng/mL). (A) Schematic of CAR T cell generation. (B) Expression of CD62L and CD44 on $CD8^+NGFR^+$ T cells at day 6 post-activation. Representative FACS plot (left) or pooled data (mean ± SEM; right) from n = 5 experiments. ***$p < 0.001$, *$p < 0.05$ paired t test. (C) Proportion of $CD8^+NGFR^+$ cells with a T_{SCM} phenotype (defined by gating as in (B) following culture in indicated cytokine combinations). Data represent mean ± SD of triplicate cultures from a representative experiment. (D–F) At day 6 post-activation, $CD8^+NGFR^+$ CAR T cells were FACS sorted into T_{EM}, T_{CM}, and T_{SCM} populations following culture with IL-2/IL-7 or IL-7/IL-15 and their transcriptome analyzed by RNA-seq. (D) Principal-component analysis (PCA) plot based upon the top 100 most variable genes. (E) Heatmap of indicated genes. (F) GSEA plots showing enrichment for a gene-set isolated from $TCF7^+$ cells and previously indicated to be responsive to immune-checkpoint blockade.[20] (G-I) At day 6 post-activation, anti-Her2 CAR T cells were cocultured with E0771-Her2 or E0771 parental tumor cells for 3 consecutive days. Supernatants were analyzed for their expression of IFN-γ at 1 day and 3 days postinitiation of coculture (G), and the $CD8^+NGFR^+$ CAR T cell phenotype was determined at the end of the experiment. (H and I) Data represent the mean ± SD of triplicate conditions from a representative experiment (I) or concatenated FACS plots from these 3 cocultures (H). **$p < 0.01$ paired t test.

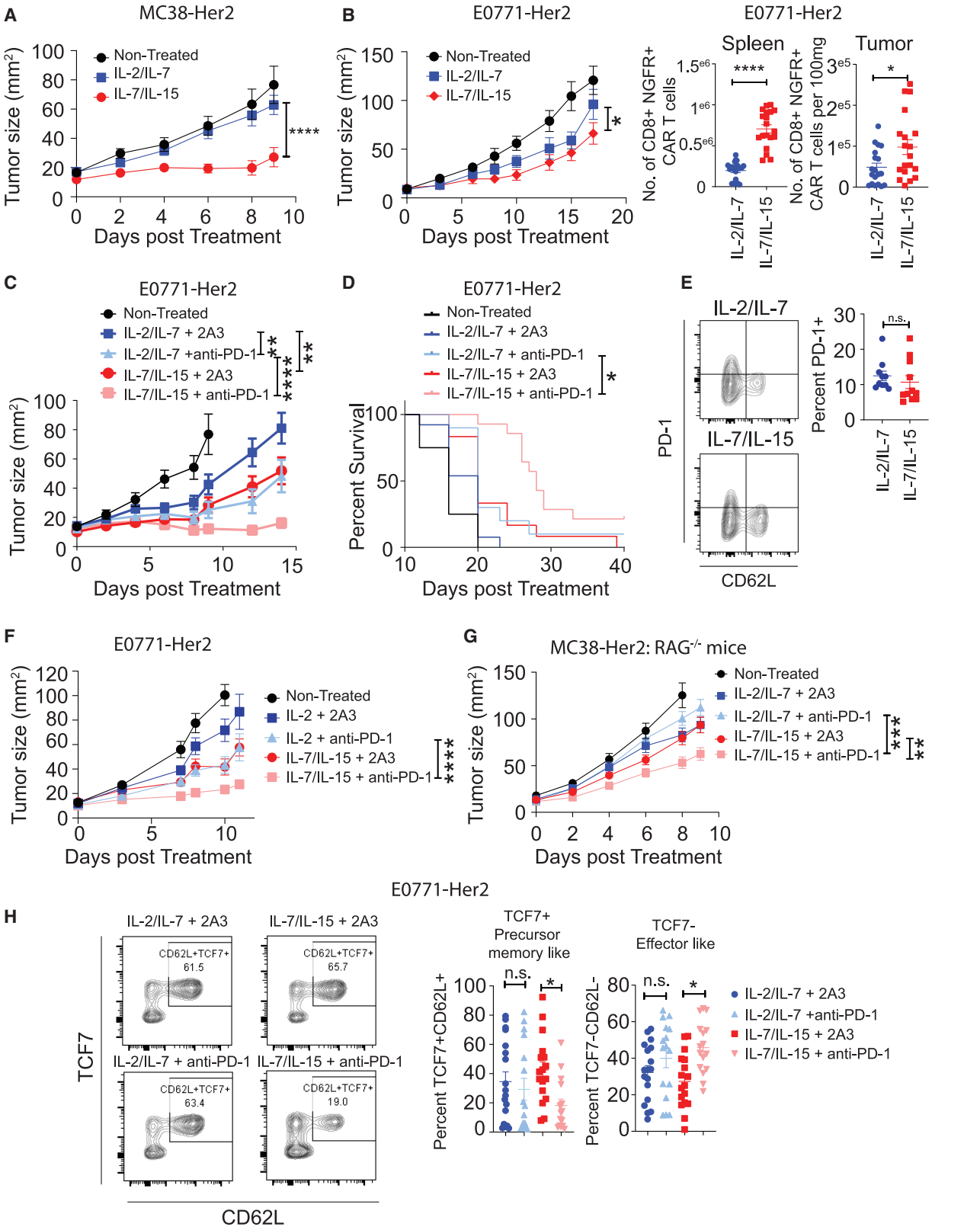

(legend on next page)

IL-7/IL-15 significantly enhanced the proportion of T_{SCM} cells relative to IL-2/IL-7-generated cells, particularly at day 7, the time point at which CAR T cells were used for functional analyses (Figure 1C). Notably, culturing of CAR T cells in IL-2, IL-7, and IL-15 or IL-2 alone resulted in levels of T_{CM} and T_{SCM} cells equivalent to cells cultured with IL-2 and IL-7, indicating that IL-2 was the dominant cytokine under these conditions and overcame the benefits of IL-15 in promoting the emergence of T_{SCM} cells (Figures S1F and 1C). To investigate the transcriptional signature of CAR T cell subsets, including the putative T_{SCM} population, we used fluorescence-activated cell sorting (FACS) for $CD8^+$ T_{EM}, T_{CM}, and T_{SCM} cells cultured in either IL-2/IL-7 or IL-7/IL-15 and performed RNA sequencing (RNA-seq). This analysis revealed that these populations clustered predominantly based upon their cytokine preconditioning rather than their cell-surface phenotype (Figure 1D). Further analysis revealed that cells cultured in IL-7 and IL-15 exhibited increased expression of memory-associated genes, including *Tcf7*, *Il7r*, *Sell*, *Foxo1*, *S1pr1*, *Lef*, and *Id3*, and these genes were among the most highly differentially expressed genes when comparing IL-7/IL-15 CAR T_{CM} cells versus IL-2/IL-7 CAR T cells of the same phenotype (Figure 1E). Gene set enrichment analysis (GSEA) analysis revealed that IL-7/IL-15 CAR T cells and the T_{SCM} population, in particular, were enriched for a gene signature previously associated with cells that are highly responsive to immune-checkpoint blockade (Figure 1F).[20] Generation of human anti-Lewis-Y CAR T cells, a clinically relevant CAR T cell product (ClinicalTrials.gov: NCT03851146), with IL-7/IL-15 as opposed to IL-2/IL-7, did not modulate the CAR T cell phenotype in terms of proportions of $CD4^+$ or $CD8^+$ T cells or proportions of $CD45RA^+$ or $CD45RO^+$ T cells (Figure S2A). However, preconditioning of anti-Lewis-Y CAR T cells with IL-7/IL-15 did enhance the expression of similar memory-related genes, as observed with murine CAR T cells, with particular differences observed in the $CD45RA^+$ population (Figures S2B and S2C). Notably, IL-7/IL-15 preconditioning of human CAR T cells also enriched for a gene signature previously reported to associate with positive responses to immune-checkpoint blockade (Figure S2D) and which was also enriched in murine CAR T cells cultured in IL-7 and IL-15 (Figure S2E).[19] To assess the functionality of IL-2/IL-7 versus IL-7/IL-15 murine CAR T cells over multiple rounds of antigen stimulation, we cocultured CAR T cells generated with each of these cytokine cocktails with E0771-Her2 tumor cells over 3 subsequent days. Whereas IL-2/IL-7 CAR T cells secreted significantly higher levels of IFN-γ after one round of coculture with tumor cells, they rapidly lost the capacity to produce this cytokine after multiple rounds of stimulation (Figure 1G). Conversely, IL-7/IL-15 CAR T cells elicited greater IFN-γ production upon subsequent rounds of coculture with $Her2^+$ tumor cells, indicating that whereas IL-2/IL-7 CAR T cells elicited greater effector function initially, IL-7/IL-15 CAR T cells exhibited enhanced capacity to differentiate into effector cells upon repeated antigen stimulation through the CAR. Notably, both IL-2/IL-7 and IL-7/IL-15 CAR T cells showed the potential to upregulate the immune-checkpoints PD-1 and TIM-3 upon coculture with Her2-expressing tumor cells, suggesting that they may be amenable to adjuvant treatment with immune-checkpoint inhibitors (Figures 1H and 1I).

Culturing CAR T Cells in IL-7 and IL-15 Enhances Their Responsiveness to Anti-PD-1 *In Vivo*

We next assessed the *in vivo* functionality of IL-7/IL-15 anti-Her2 CAR T cells relative to IL-2/IL-7 CAR T cells. To investigate this, we preconditioned anti-Her2 CAR T cells in IL-7 and IL-15 or IL-2 and IL-7 and treated E0771-Her2 or MC38-Her2 tumor-bearing mice having confirmed that both tumor cell lines expressed PD-L1 (Figure S3). We first tested this in the MC38-Her2 tumor model, where we have previously observed that CAR T cell responses are limited using our standard IL-2/IL-7 preconditioning protocol.[22] We observed that IL-7/IL-15 CAR T cells exhibited significantly greater therapeutic efficacy than IL-2/IL-7 CAR T cells (Figure 2A). However, in the E0771-Her2 tumor model, CAR T cells generated in IL-7/IL-15 elicited only a modest, yet statistically significant, increase in efficacy relative to IL-2/IL-7 CAR T cells (Figure 2B). This was despite the fact that preconditioning of anti-Her2 CAR T cells with IL-7 and IL-15 significantly increased the number of CAR T cells in the spleens (3-fold, $p < 0.01$) and tumors (2-fold, $p < 0.05$) of E0771-Her2 tumor-bearing mice (Figure 2B). Further analysis of memory-associated genes revealed that tumor-infiltrating CAR T cells analyzed at day 9 post-treatment exhibited similar expression of the transcription factors TCF7, IRF4, and Tbet regardless of the cytokine preconditioning regimen utilized (Figure S4A). Moreover, IL-2/IL-7 and IL-7/IL-15 CAR T cells exhibited similar expression of proteins related to effector function (PD-1, TIM-3, and Ki-67), with the exception of granzyme B, which was more highly expressed by IL-2/IL-7 CAR T cells (Figure S4A). We next investigated whether IL-7/IL-15 CAR T cells exhibited enhanced responses to anti-PD-1 adjuvant therapy. Whereas treatment with anti-PD-1 alone had no effect on E0771-Her2 tumor growth, consistent with our previous observations[14,16] (Figure S4B), it significantly enhanced

Figure 2. Preconditioning CAR T Cells with IL-7/IL-15 Leads to Enhanced Anti-Tumor Efficacy When Combined with Anti-PD-1

(A–F and H) C57BL/6 Her2 transgenic (Tg) or (G) $RAG^{-/-}$ mice were injected subcutaneously with 2×10^5 MC38-Her2 CAR T cells or with 2×10^5 E0771-Her2 tumor cells into the fourth mammary fat pad and treated with anti-Her2 CAR T cells, generated as per Figure 1. 1×10^7 CAR T cells were injected intravenously on days 7 and 8 (E0771-Her2) or 5 and 6 (MC38-Her2) following total body irradiation (4 Gy or 0.5 Gy, respectively). Mice were treated with 50,000 U of IL-2 on days 0–4 post-CAR T cell treatment and with either anti-PD-1 (200 μg/mouse) or 2A3 isotype control on days 0, 4, 8, and 12 post-treatment. (A, B, F, and G) Tumor growth, shown as the mean ± SEM of n = 6–8 mice per group. $^{**}p < 0.01$, $^{****}p < 0.0001$ two-way ANOVA. (B) 9 days post-treatment, spleens and tumors were excised, and the number of $CD8^+NGFR^+$ CAR T cells in the indicated organs was determined by flow cytometry. Data represent the mean ± SEM of 19–20 mice per group from 3 replicate experiments. $^{****}p < 0.0001$, $^{*}p < 0.05$ unpaired t test. (C) Tumor growth, shown as the mean ± SEM of 12–14 mice per group from 2 pooled experiments. $^{**}p < 0.01$, $^{****}p < 0.0001$ two-way ANOVA. (D) Survival of mice with end point defined as when tumors exceeded 100 mm^2. $^{*}p < 0.05$ log rank test. (E and H) Expression of CD62L, PD-1, and TCF7 within $CD8^+NGFR^+$ CAR T cells. FACS plots represent concatenated data from n = 8 mice. Pooled data represent the mean ± SEM of 10–17 mice per group from 2 to 3 replicate experiments. $^{*}p < 0.05$ one-way ANOVA.

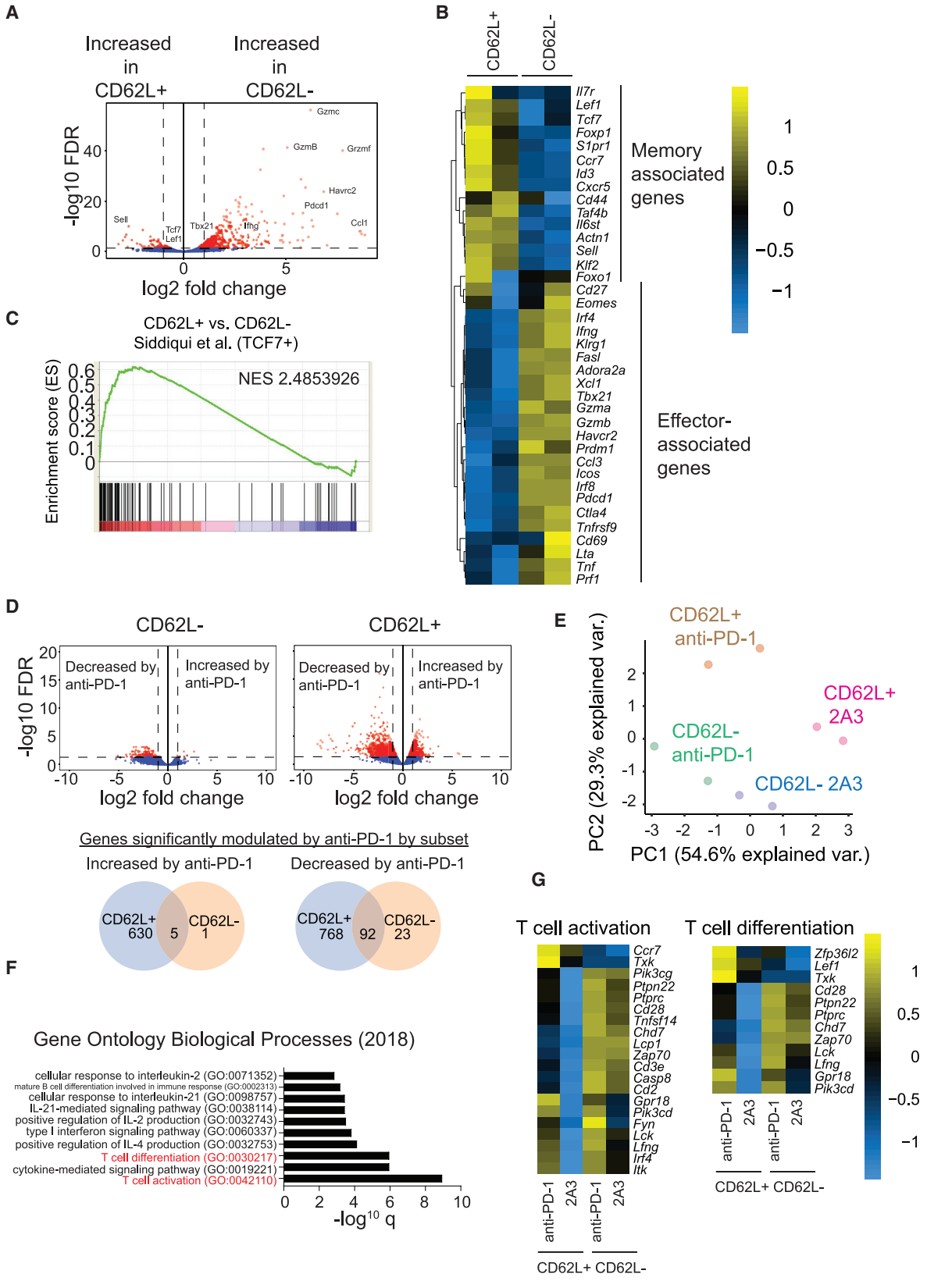

(legend on next page)

the therapeutic efficacy of IL-2/IL-7 CAR T cells in terms of growth inhibition (Figure 2C) but with no statistically significant effect on survival (Figure 2D). In line with our hypothesis, effects mediated by anti-PD-1 adjuvant therapy were significantly greater following preconditioning of CAR T cells with IL-7/IL-15, leading to significantly enhanced tumor growth inhibition and long-term survival of mice (Figures 2C and 2D). This was despite similar levels of PD-1 expression on intratumoral $CD8^+$ CAR T cells following preconditioning with IL-2/IL-7 or IL-7/IL-15 (Figure 2E). Similarly, IL-7/IL-15 CAR T cells exhibited enhanced responsiveness relative to CAR T cells preconditioned in IL-2 alone (Figure 2F). We next examined this effect in the MC38-Her2 tumor model. To confirm that the effects of anti-PD-1 were due to activation of CAR T cells (and not endogenous T cell activation), we utilized $RAG^{-/-}$ mice to investigate this effect. The efficacy of CAR T cells was reduced in $RAG^{-/-}$ mice (Figure 2G) relative to wild-type (WT) mice (Figure 2A), likely as a result of more aggressive tumor growth due to lack of endogenous T cell anti-tumor immunity. However, these experiments revealed that IL-7/IL-15 CAR T cells elicited significantly greater therapeutic effects than IL-2/IL-7 CAR T cells when combined with anti-PD-1 adjuvant therapy (Figure 2G).

To investigate the mechanism by which IL-7/IL-15 CAR T cells exhibited enhanced responses to anti-PD-1, we assessed the numbers and differentiation status of CAR T cells at the tumor site. In line with our previous observations with IL-2/IL-7 CAR T cells,[14,16] PD-1 blockade did not significantly affect the numbers of CAR T cells in the spleens or tumors of treated mice (Figure S4C). To interrogate effects on differentiation status, we analyzed the proportion of $CD62L^+TCF7^+$ cells following anti-PD-1 therapy, since previous reports have indicated that $CD62L^+TCF7^+$ cells are the most responsive to immune-checkpoint blockade in the context of conventional immunotherapy.[23] Interestingly, we observed a significant reduction in the proportion of $CD62L^+TCF7^+$ cells following treatment of IL-7/IL-15 CAR T cells, but not IL-2/IL-7 CAR T cells, with anti-PD-1 adjuvant therapy (Figure 2H). This was concomitant with an increase in the proportion of $CD62L^-TCF7^-$ effector-like CAR T cells in the context of PD-1 blockade (Figure 2H), suggesting that $TCF7^+$ cells may be more prone to differentiation into effector-like cells following IL-7/IL-15 preconditioning. Indeed, stimulation of CAR T cells *in vitro* led to a reduction in TCF7 expression at the transcript and protein level (Figures S4D and S4E), indicating that CAR T cells decrease TCF7 expression following activation and differentiation.

The $CD62L^+TCF7^+$ CAR T Cell Subset Is the Most Responsive to Anti-PD-1 Adjuvant Therapy

Having observed that anti-PD-1 treatment led to a significant reduction in the proportion of $CD62L^+TCF7^+$ cells when CAR T cells were generated with IL-7/IL-15, we examined whether these cells were responding to anti-PD-1 therapy at the transcriptional level. To assess this, we generated IL-7/IL-15 anti-Her2 CAR T cells, treated E0771-Her2 tumor-bearing mice, and FACS sorted intratumoral $CD62L^+$ and $CD62L^-CD8^+$ CAR T cells at day 9 post-treatment following 48 h of adjuvant PD-1 therapy (or isotype control; antibody treatment at day 7). RNA-seq on the $CD62L^+$ and $CD62L^-$ subsets validated that the $CD62L^-$ cells elicited an increased expression of several genes associated with CAR T cell effector function, such as IFN-γ and granzyme B (Figures 3A and 3B; Table S1). As expected, this analysis also revealed that $CD62L^+$ CAR T cells expressed higher levels of memory-associated genes, including *Tcf7*, *Sell*, *Id3*, and *Lef1* (Figures 3A and 3B; Table S1). GSEA analysis revealed that the $CD62L^+$ subset exhibited a phenotype similar to a previously described endogenous $CD8^+$ T cell population that was responsive to conventional immune-checkpoint blockade (Figure 3C).[20] Consistent with this, we observed that the vast majority of transcriptional changes following anti-PD-1 therapy occurred within the $CD62L^+$ population (Figures 3D and 3E), and analysis of these differentially expressed genes following anti-PD-1 therapy revealed an enrichment for genes within the gene ontology (GO) terms "T cell activation" and "T cell differentiation" (Figure 3F). Notably, within the $CD62L^+$ population, we also observed increased transcription of T cell receptor (TCR)-induced transcription factors *Irf4*, *Nfatc1*, and *Batf* and increased expression of T cell activation genes, including *Cd69*, *Pdcd1*, *Havcr2*, and *Ifng*. Taken together, these data suggest that the $CD62L^+$ population was the most responsive to anti-PD-1 therapy when CAR T cells were preconditioned with IL-7 and IL-15, leading to the differentiation and activation of these cells (Figure 3G). Therefore, these data suggest that IL-7/IL-15 preconditioning enforces a unique transcriptional profile in $CD62L^+TCF7^+$ cells (Figures 3E and 3F), leading to enhanced differentiation of these cells following anti-PD-1 adjuvant therapy (Figures 3D–3G).

Preconditioning CAR T Cells with IL-7/IL-15 Leads to Enhanced Effector Functions When Combined with Anti-PD-1 Treatment *In Vivo*

To assess further the mechanism underlying the enhanced response of IL-7/IL-15 CAR T cells to anti-PD-1 therapy, we performed an analysis of the expression of effector proteins (IFN-γ, TNF, Ki-67, granzyme B,

Figure 3. The $CD8^+CD62L^+$ CAR T Cell Population Elicits the Majority of Transcriptional Changes Following PD-1 Blockade

C57BL/6 Her2 Tg mice were injected with 2×10^5 E0771-Her2 tumor cells into the fourth mammary fat pad and treated with IL-7/IL-15-generated anti-Her2 CAR T cells as per Figure 2. Mice were treated on day 7 with anti-PD-1 (200 μg/mouse) or 2A3 isotype control, and on day 9, tumors were excised, and $CD8^+NGFR^+CD62L^+$ and $CD8^+NGFR^+CD62L^-$ were isolated by FACS sorting. Transcriptional changes were analyzed by RNA-seq. Data represent a pool of cells obtained from 3 mice for each biological replicate. (A) Differential gene-expression analysis; genes in red indicate significance based upon an FDR of <0.05. (B) Gene expression by heatmap for indicated cell populations in mice treated with 2A3 isotype control. (C) GSEA plot showing enrichment for genes upregulated in $CD62L^+$ (relative to $CD62L^-$) compared to a gene set identified in $TCF7^+$ cells responsive to immune-checkpoint blockade.[20] (D) Differential gene-expression analysis following anti-PD-1 treatment in $CD62L^-$ and $CD62L^+$ cells. Volcano plots (top) and Venn diagram showing overlapping genes (bottom) with significance cutoff set at FDR < 0.05. (E) Principal component plot based upon the top 1,000 most variable genes. (F and G) Enriched pathways within the gene ontology (GO) biological processes database based upon differentially expressed genes within $CD62L^+$ cells following anti-PD-1 treatment. (F) Most significantly enriched Gene Ontology (GO) pathways (G) Heatmaps indicate gene expression within selected GO pathways.

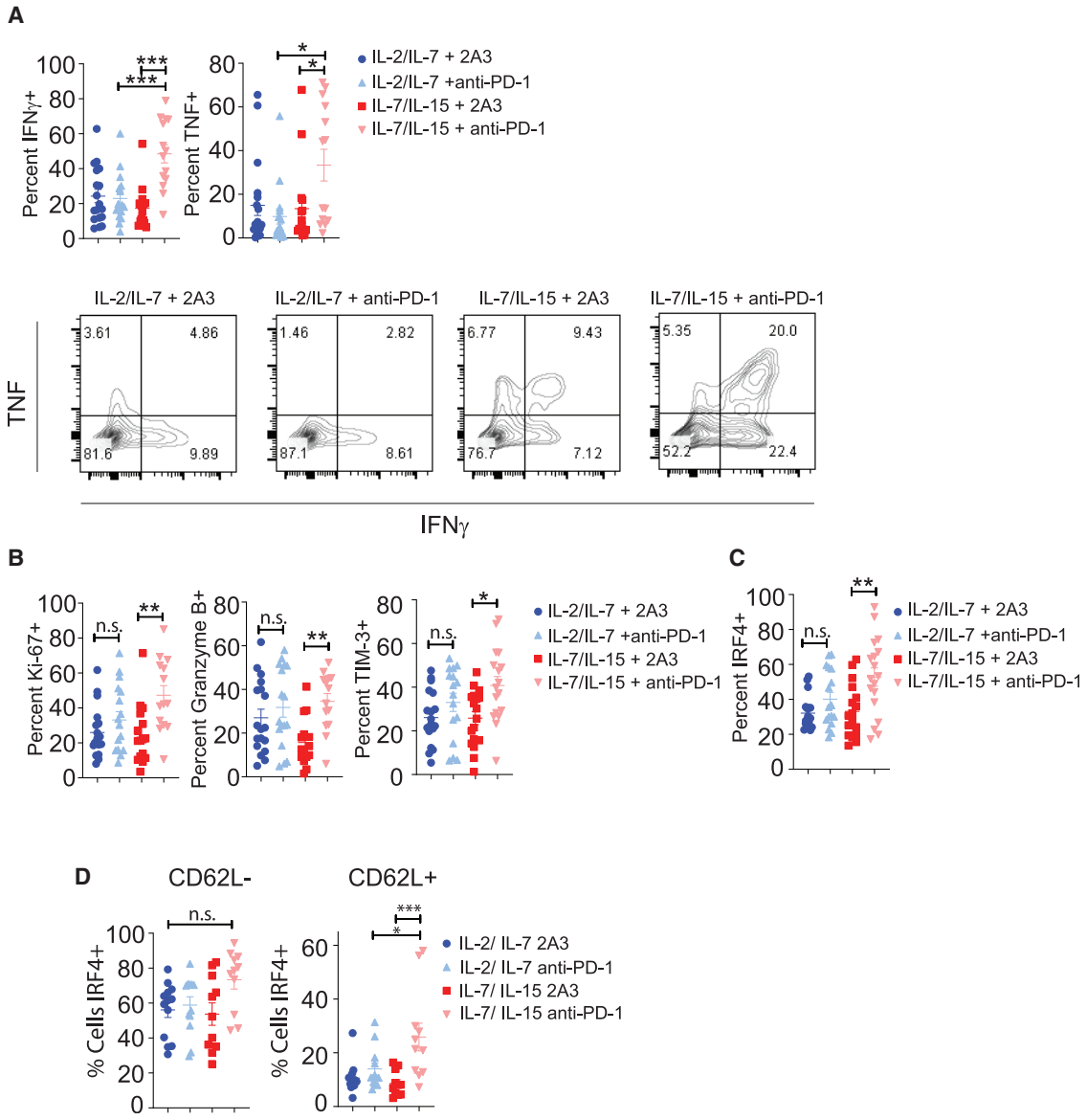

Figure 4. IL-7/IL-15 Preconditioned CAR T Cells Elicit a More Potent Effector Response Following Anti-PD-1 Treatment

C57BL/6 Her2 Tg mice were injected with 2 × 10^5 E0771-Her2 tumor cells into the fourth mammary fat pad and treated with anti-Her2 CAR T cells as per Figure 2, having been generated with IL-2/IL-7 or IL-7/IL-15. At day 9 post-treatment, tumors were excised, and tumor-infiltrating $CD8^+NGFR^+$ CAR T cells were analyzed by flow cytometry. (A) The expression of IFN-γ and TNF following 3 h of PMA (5 ng/mL) and ionomycin (1 μg/mL) in the presence of GolgiPlug and GolgiStop. Top: data shown as mean ± SEM of 14–18 mice per group from 3 replicate experiments. *$p < 0.05$, ***$p < 0.001$, one-way ANOVA. Bottom: concatenated data from 8 mice per group. (B and C) The expression of (B) Ki-67, granzyme B, and TIM-3 and (C) IRF4 in $CD8^+NGFR^+$ CAR T cells. Data shown as mean ± SEM of 14–18 mice per group from 3 replicate experiments. *$p < 0.05$, **$p < 0.01$, one-way ANOVA. (D) The expression of IRF4 in $CD62L^-$ and $CD62L^+$ subsets. Data are from concatenated mice from a representative experiment of n = 2. Bottom: pooled data from 11–13 mice per group from 2 individual experiments. *$p < 0.05$, ***$p < 0.001$, one-way ANOVA.

TIM-3) by $CD8^+$ CAR T cells by flow cytometry at day 9 post-treatment (Figures 4A and 4B). Consistent with our previous observations at this time point,[16] we observed that PD-1 blockade did not significantly enhance production of these effector proteins by CAR T cells when they were preconditioned with IL-2/IL-7. However, IL-7/IL-15 CAR T cells exhibited greater responsiveness to adjuvant therapy, leading to significantly greater expression of IFN-γ and TNF following phorbol 12-myristate 13-acetate (PMA)/ionomycin treatment relative to IL-2/IL-7 CAR T cells treated with anti-PD-1 (Figure 4A). To test this in the context of CAR-specific stimulation (as opposed to PMA/ionomycin), we evaluated IFN-γ production of $CD8^+$ T cells following *ex vivo* stimulation with an anti-CAR-stimulating antibody. Consistent

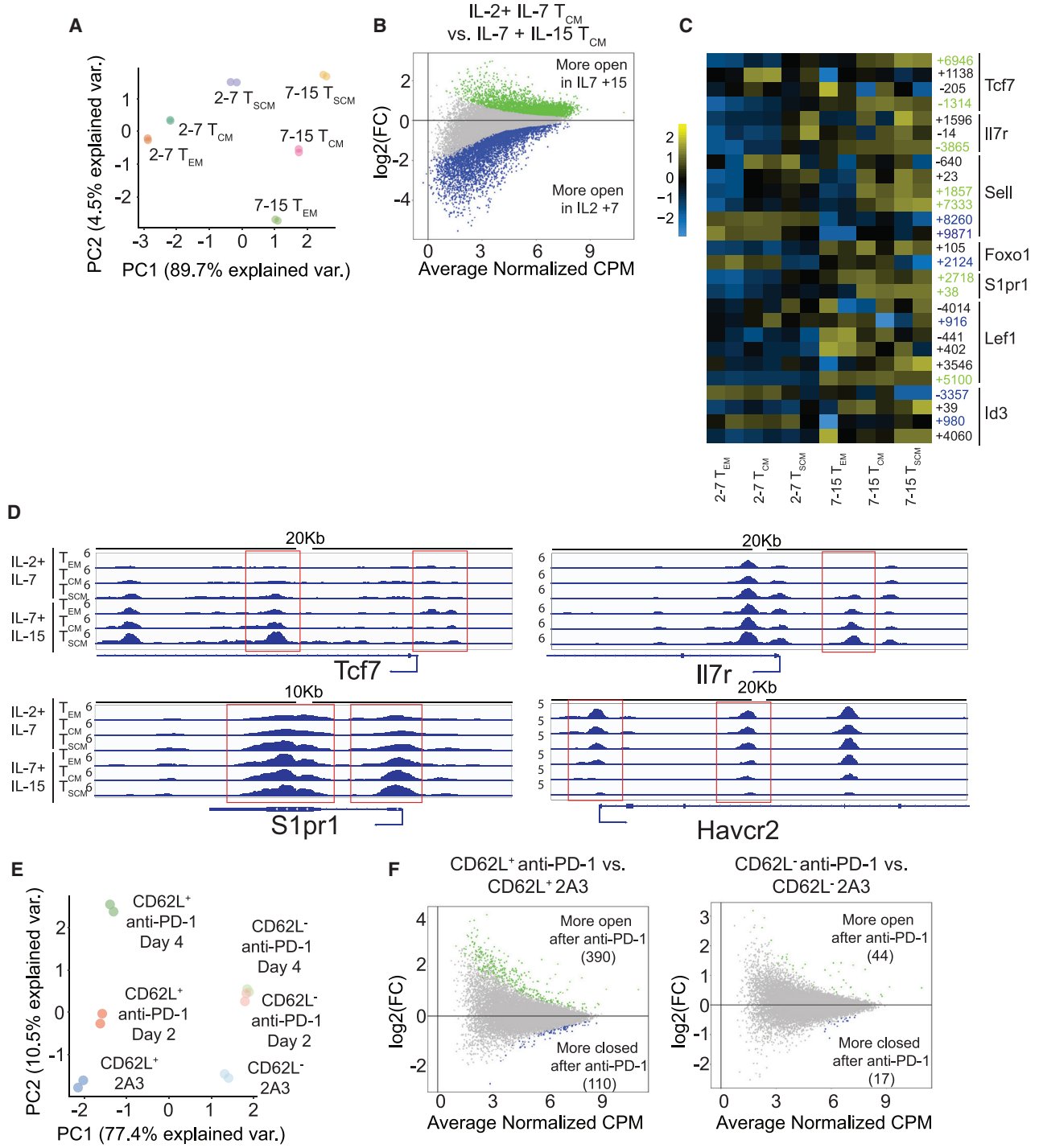

Figure 5. IL-15 Preconditioning Results in a Favorable Epigenetic Landscape for Enhanced Effector Functions Following PD-1 Blockade

Anti-Her2 CAR T cells were generated in IL-2 (100 U/mL) and IL-7 (200 pg/mL) or IL-7 and IL-15 (10 ng/mL). (A–D) At day 6 post-activation, $CD8^+NGFR^+$ CAR T cells were FACS sorted into T_{EM}, T_{CM}, and T_{SCM} populations and their genome accessibility analyzed by ATAC-seq. (A) PCA plot based on the 5,000 most variable peaks. (B and C) Analysis was restricted to sites within −5 kb or +10 kb of TSS. (B) MA plot of log2 fold change (FC) differences in accessibility peaks between T_{CM} CAR T cells generated with IL-2/IL-7 or IL-7/IL-15 versus the mean of normalized log CPM. Colored peaks are statistically significant. (C) Heatmap of normalized log CPM for peaks associated with individual genes. Green and blue indicate sites significantly more/less accessible, respectively, after IL-15 treatment. Numbers indicate position of peak relative to TSS. (D)

(legend continued on next page)

with effects observed with PMA/ionomycin, IFN-γ production was highest in mice treated with IL-7/IL-15 preconditioned CARs and anti-PD-1 (Figure S5). Moreover, PD-1 blockade resulted in significant increases in Ki-67, granzyme B, and TIM-3 expression in IL-7/IL-15 CAR T cells, but not IL-2/IL-7 control CAR T cells, further confirming the increased responsiveness of these CAR T cells to anti-PD-1 adjuvant therapy (Figure 4B). We also analyzed the phenotype of tumor-infiltrating $CD4^+$CAR T cells given recent data indicating the clinical importance of this subset. Preconditioning CAR T cells with IL-7/IL-15 led to an increase in the $CD8^+$:$CD4^+$ CAR T cell ratio (Figure S6A), but this was explained by an increased number of $CD8^+$ CAR T cells (Figure 2B), whereas numbers of $CD4^+$ CAR T cells were unaffected. However, the proportion and number of $CD4^+$ CAR T cells were significantly diminished following anti-PD-1 therapy when CAR T cells were generated with IL-7/IL-15 but not IL-2/IL-7. This was concomitant with a reduction in the proportion of $CD62L^+TCF7^+CD4^+$ CAR T cells (Figure S6B) and an increased activation status of $CD4^+$ CAR T cells following anti-PD-1 blockade, indicated by their increased expression of IFN-γ, TNF, Ki-67, and granzyme B (Figures S6C and S6D). Similarly to $CD8^+$ CAR T cells, these parameters were only modulated by PD-1 blockade when CAR T cells were preconditioned with IL-7/IL-15 but not IL-2/IL-7.

To assess further the impact of cytokine preconditioning on the differentiation of $CD8^+$ CAR T cells, we analyzed expression of IRF4, a transcription factor known to play an important role in $CD8^+$ T cell differentiation and effector function.[24] With IL-7/IL-15 CAR T cells, PD-1 blockade resulted in a significant increase in the expression of IRF4 (Figure 4C). Notably, this increase in expression of IRF4 was most pronounced within the $CD62L^+$ population, consistent with our data at the transcriptional level (Figures 3G and 4D). Taken together, our data indicate that the preconditioning of CAR T cells with IL-7 and IL-15 leads to enhanced anti-tumor activity when combined with anti-PD-1 adjuvant therapy *in vivo*, and this effect was associated with an increased responsiveness of $CD8^+CD62L^+TCF7^+$ cells. Subsequently, these CAR T cells exhibited significantly enhanced expression of key effector molecules, including IFN-γ and TNF, which we have previously shown to be important for the efficacy of CAR T cells in solid tumors.[16,25]

Preconditioning CAR T Cells with IL-15 Promotes a Favorable Epigenetic Landscape within $CD8^+$ CAR T Cells for Responses to Anti-PD-1

To understand further the mechanism by which IL-15 preconditioning enhances CAR T cell responses to anti-PD-1 adjuvant therapy, we analyzed the effect of IL-15 on the epigenome of $CD8^+$ CAR T cells. We first assessed this in terms of the CAR T cells being injected into mice following FACS sorting of T_{EM}, T_{CM}, and T_{SCM} populations of CAR T cells generated with IL-2/IL-7 or IL-7/IL-15 as per Figures 1D–1F. Principal-component analysis (PCA) of the 5,000 most variably accessible sites revealed that similarly to the transcriptome analysis, cells clustered based on their cytokine preconditioning to a greater extent than their phenotype defined by their expression of CD62L and CD44 (Figure 5A). Analysis of differentially accessible sites in T_{CM} CAR T cells generated in IL-2/IL-7 or IL-7/IL-15 revealed that there were 6301 significantly more accessible and 5,777 significantly less accessible peaks following culture in IL-7 and IL-15 (Figure 5B). Interestingly, we observed that some memory-associated genes, such as *Tcf7* and *S1pr1*, displayed multiple sites that were more accessible following IL-15 treatment (Figures 5C and 5D). Indeed, analysis of differential accessible regions between T_{CM} cells generated in either IL-2/IL-7 or IL-7/IL-15 at a range of gene loci revealed that IL-7/IL-15 preconditioning resulted in an epigenetic profile that was more similar to stem-like cells that have previously been shown to be highly responsive to PD-1 blockade.[26] This included increased accessibility of memory genes and decreased accessibility of inhibitory receptors, such as *Havcr2* (Figures 5C, 5D, and S7A). We next analyzed the chromatin landscape of CAR T cells *ex vivo* 9 days following treatment. Analysis of IL-2/IL-7 and IL-7/IL-15-generated CAR T cells recovered from the spleens of E0771-Her2 tumor-bearing mice revealed that IL-2/IL-7-generated CAR T cells retained their increased accessibility of genes associated with terminal differentiation, such as *Havcr2* and *Klrg1* (Figure S7B). We next explored the epigenetic landscape of tumor-infiltrating CAR T cells. We focused upon CAR T cells generated with IL-7/IL-15 and isolated the $CD62L^+$ and $CD62L^-$ subsets following treatment with anti-PD-1 for either 2 or 4 days. PCA of the top 5,000 differentially regulated peaks revealed that the $CD62L^+$ and $CD62L^-$ subsets exhibited distinct epigenetic profiles as expected (Figure 5E). In the absence of adjuvant treatment, $CD62L^-$ cells possessed regions of increased accessibility at peaks associated with effector-related genes, such as *Ifng*, *Tnf*, and *Irf4*, relative to $CD62L^+$ cells, likely indicative of active transcription of these genes. Following anti-PD-1 treatment, epigenetic changes were more marked in the $CD62L^+$ subset, with 500 significantly altered peaks compared to 61 in $CD62L^-$ CAR T cells (Figures 5E and 5F). Notably, changes in the $CD62L^+$ cells were more marked and prolonged, since very little chromatin arrangements occurred within the $CD62L^-$ subset after 2 days of treatment (Figure 5E), likely indicative of differentiation toward an effector-like phenotype early after treatment. These data support the notion that preconditioning of CAR T cells with IL-7/IL-15 leads to a favorable epigenetic profile for enhanced persistence and responsiveness to anti-PD-1 and that, within tumors, memory-like CAR T cells, marked by their expression of CD62L and TCF7, are the most responsive to anti-PD-1 in terms of transcriptional and epigenetic changes.

DISCUSSION

Recent studies investigating the mechanism underlying immune-checkpoint blockade therapy have shown that within $CD8^+$ T cells,

Accessibility tracks for selected genes and indicated cell types. (E and F) C57BL/6 Her2 Tg mice were injected with 2×10^5 E0771-Her2 tumor cells into the fourth mammary fat pad and treated with IL-7/IL-15-generated anti-Her2 CAR T cells and CAR T cells FACS sorted at day 9 post-treatment as per Figure 3. (E) PCA plot based on the 5,000 most variable peaks. (F) MA plot of log 2FC differences in accessibility peaks between $CD62L^+$ or $CD62L^-$ CAR T cells treated with either 2A3 or anti-PD-1 on day 5 post-treatment versus the mean of normalized log CPM.

a less differentiated $CD62L^+TCF7^+$ population is the most responsive to immune-checkpoint blockade and correlates with improved therapeutic responses.[19,20,27] However, this has not been investigated in the context of CAR T cell responses, which are of high importance given the number of clinical trials proposing to utilize the combination of CAR T cells and immune-checkpoint inhibitors.[5,6] Standard CAR T cell culturing conditions used in the clinic result in the generation of a CAR T cell product with an effector/exhausted phenotype, which has limited persistence[28] and is unlikely to be optimally responsive to immune-checkpoint blockade. Whereas biomarkers of persistence, including a $CD45RA^+CD27^+$ population,[28] have been shown to be prognostic for engraftment and persistence, no such biomarkers currently exist for predicting CAR T cell responses to immune-checkpoint blockade.

Previous studies have shown that preservation of CAR T cells in the T_{CM} phenotype results in superior engraftment and anti-tumor effects.[7,8] This can be achieved through alteration of the cytokine milieu for CAR T cell culture;[10,29–31] pharmacological inhibition of key signaling pathways, such as Akt,[32] or epigenetic modulation.[11,12,33] Consistent with this, our current study showed that preservation of CAR T cells in a more stem-like phenotype prior to adoptive transfer resulted in enhanced engraftment and numbers of CAR T cells infiltrating tumors. Whereas previous studies have shown that IL-15 can enhance the efficacy of adoptive cellular therapy by enhancing a T_{CM} phenotype,[10] due to its inhibition of mammalian target of rapamycin (mTOR) within transferred T cells,[31] our study demonstrates that IL-15 initiates a transcriptional and epigenetic program associated with an enhanced capacity to respond to PD-1 blockade. Thus, preconditioning of CAR T cells with IL-15 consequently enhances their anti-tumor functionality when combined with anti-PD-1 adjuvant therapy. This is of high clinical relevance given that a number of ongoing trials are investigating the combination of CAR T cells and adjuvant immune-checkpoint blockade using standard CAR T cell culturing conditions, which our data suggest are likely to lead to suboptimal responses to anti-PD-1 (ClinicalTrials.gov: NCT03287817, NCT02926833, and NCT02706405). More recently, improved methods to generate stem cell-like CAR T cells have been developed,[34] but these are yet to be utilized in conjunction with strategies designed to block PD-1.

Treatment of CAR T cells with IL-7 and IL-15 *in vitro* led to transcriptional changes that were in alignment with previously reported gene sets for T cell populations that respond to immune-checkpoint blockade.[19,20,27] Notably, we observed that not only did IL-15 enhance the proportion of cells expressing a T_{CM} phenotype ($CD62L^+$), but also, comparison of T_{CM} cells generated in IL-2/IL-7 versus IL-7/IL-15 revealed that IL-7/IL-15-generated T_{CM} cells exhibited increased expression of genes associated with a positive response to PD-1 blockade, such as *Tcf7*, relative to IL-2/IL-7-generated T_{CM} counterparts. Thus, IL-15 enhanced the T_{CM} phenotype both quantitatively and qualitatively, and so analysis of the cell-surface phenotype of a CAR T cell product alone may be insufficient to predict their responsiveness to immune adjuvants. An interesting observation from analysis of the epigenome of CAR T cells conditioned with IL-15 was that it selectively enhanced the accessibility of certain memory-related genes, such as *Il7r* and *Tcf7*, whereas other genes, such as *Foxo1*, were not affected. This suggests that rational combinations between IL-15 and epigenetic modifiers that target these loci may potentially synergize and further enhance CAR T cell persistence.

IL-7/IL-15 preconditioning enhanced the capacity of $CD62L^+TCF7^+$ CAR T cells to respond to anti-PD-1 therapy, both transcriptionally and epigenetically, resulting in significant increases in key effector proteins, including IFN-γ, TNF, Ki-67, and granzyme B. We have previously shown that both IFN-γ and TNF are critical cytokines for CAR T cell-mediated control of solid tumors *in vivo*,[16,25] suggesting that the capability of IL-7/IL-15-preconditioned CAR T cells to secrete enhanced levels of these cytokines may contribute to their enhanced effector function. These results are consistent with results observed by Siddiqui et al.,[20] whereby depletion of the $TCF7^+$ subset was shown to abrogate responses to conventional immune-checkpoint blockade.

Notably, the increased expression of IRF4 within the $CD62L^+$ subset following anti-PD-1 is indicative of the increased activation/differentiation of these cells. IRF4 expression is associated with effector cell functions, such as IFN-γ production, but has also been shown to promote terminal T cell differentiation through repression of the transcription factor TCF7.[24] This may explain why treatment with PD-1 is associated with a loss of less differentiated $CD62L^+TCF7^+$ cells and potentially why PD-$1^{-/-}$ T cells have been shown to be prone to terminal differentiation in a chronic viral setting.[35] Thus, transient and/or tumor microenvironment-specific modulation of immune checkpoints may be preferable in the setting of CAR T cell therapy to preserve their less differentiated phenotype and maximize their ability to proliferate and differentiate within the tumor microenvironment. Taken together, our data suggest that preservation of CAR T cells in a less differentiated $CD62L^+TCF7^+$ phenotype through the use of IL-15 conditioning can enhance both their persistence and responsiveness to immune-checkpoint adjuvant therapies.

MATERIALS AND METHODS

Cell Lines and Mice

The C57BL/6 mouse breast carcinoma cell line E0771, a gift from Prof. Robin Anderson (Olivia Newton-John Cancer Research Institute), and MC38 were engineered to express truncated human Her2, as previously described.[36] Tumor lines were also verified to be mycoplasma negative by PCR analysis. Tumor cells were grown in RPMI, supplemented with 10% fetal calf serum (FCS), 2 mM glutamine, 0.1 mM nonessential amino acids (NEAAs), HEPES, 1 mM sodium pyruvate, and penicillin/streptomycin, and used in less than 8 passages from a master stock. For assessment of CAR T cell activity *in vivo*, cells were resuspended in PBS and injected subcutaneously in a 100-μL volume (male mice; MC38-Her2) or into the fourth mammary fat pad in a 20-μL volume (female mice; E0771-Her2). C57BL/6 WT mice or C57BL/6 Her2 mice were bred in-house at the Peter

MacCallum Cancer Centre (PMCC), and RAG$^{-/-}$ mice were obtained from the Walter and Eliza Hall Institute (WEHI; Melbourne, Australia). Mice were used between 6 and 16 weeks of age. All animal experiments were performed under the approval from the PMCC Animal Experimentation Ethics Committee (number E582).

Antibodies and Cytokines

Antibodies to PD-1 (clone RMP1-14) or isotype control (clone 2A3) were purchased from Bio X Cell. For cell stimulation, anti-CD3 (clone 145-2C11) and anti-CD28 (clone 37.51) antibodies were purchased from BD Pharmingen. Recombinant human IL-2/IL-15 and murine IL-7 used for T cell stimulation were obtained from the NIH and PeproTech, respectively.

Generation of Murine CAR T Cells

Retrovirus encoding a CAR composed of an extracellular scFv-anti-human Her2 fused to the transmembrane domains of CD28 and CD3ζ was obtained from the supernatant of the GP+E86 packaging line, as previously described.[14,37] This GP+E86 anti-Her2 CAR packaging line was then further engineered to also produce retrovirus encoding a truncated human NGFR to allow tracking of transduced cells. Splenocytes were cultured in RPMI, supplemented with 10% FCS, NEAA, sodium pyruvate, glutamine, HEPES, and penicillin/streptomycin. Splenocytes were activated with anti-CD3 (0.5 μg/mL) and anti-CD28 (0.5 μg/mL) in the presence of 100 IU/mL IL-2 and 200 pg/mL IL-7 at a density of 5×10^6/mL. After 24 h, live T cells were isolated after a Ficoll centrifugation step. 4 mL of retroviral supernatant was added to each well of retronectin-coated (10 μg/mL) 6-well plates (Takara Bio). Viral supernatant was spun onto retronectin-coated plates at 1,200 × *g* for 30 min, after which T cells were resuspended in 1 mL of additional retroviral-containing supernatant, supplemented with IL-2 and IL-7, and then added to the retronectin-coated plates to give a final volume of 5 mL/well. Final T cell concentration was 5×10^6 to 10×10^6 per well. T cells were spun for 90 min, after which they were incubated overnight before repetition of the transduction process the following day. After the transduction was completed, T cells were maintained in IL-2 and IL-7, IL-7 and IL-15 (10 ng/mL), or IL-2, only containing media and cells used at days 6–8 after transduction.

Generation of Human CAR T Cells

Retrovirus encoding a second-generation scFv-anti-Lewis-Y CAR, linked to a human CD8 hinge region and cytoplasmic domains of human CD28 and CD3ζ, was obtained from the supernatant of the PG13 packaging line, as previously described.[38] Human peripheral blood mononuclear cells (PBMCs) were cultured in RPMI, supplemented with 10% FCS, NEAA, sodium pyruvate, glutamine, HEPES, and penicillin/streptomycin. PBMCs were isolated from normal buffy coats using Ficoll centrifugation and activated for 48 h with anti-human CD3 (OKT3 30 ng/mL; Ortho Biotech) and cytokines, IL-2 (100 IU/mL) and IL-7 (5 ng/mL), or IL-7 (5 ng/mL) and IL-15 (5 ng/mL). Retronectin-coated (15 μg/mL) 6-well plates (Takara Bio) were centrifuged at 1,200 × *g* for 1 h with 5 mL of retroviral supernatant added to each well. Retroviral supernatant was removed prior to the addition of activated PBMCs resuspended at a concentration of 0.5×10^6/mL in fresh 5 mL of retrovirus containing IL-2/IL-7 or IL-7/IL-15. Centrifugation at 1,200 × *g* for 1 h was performed, and cells were incubated overnight before repeating the transduction process the next day. Following transduction, cells were cultured at a density of 1.5×10^6/mL with IL-2/IL-7 or IL-7/IL-15 and FACS sorted for RNA-seq analysis at day 7.

Treatment of Tumor-Bearing Mice

C57BL/6 human Her2 transgenic mice or RAG$^{-/-}$ mice were injected in the fourth mammary fat pad with 2×10^5 E0771-Her2 cells or subcutaneously with 2×10^5 MC38-Her2 tumor cells. At day 7 (E0771-Her2) or day 5 (MC38-Her2) after tumor injection, mice were preconditioned with total-body irradiation (4 Gy E0771-Her2, 0.5 Gy MC38-Her2) prior to the administration of 1×10^7 CAR T cells on days 7 and 8. Mice were also treated with 50,000 IU IL-2 on days 0–4 after T cell transfer. Mice were treated with either isotype control (2A3) or anti-PD-1 (200 μg per mouse) on days 0, 4, 8, and 12 after T cell transfer.

Analysis of Tumor-Infiltrating Immune Subsets

For analysis of tumor-infiltrating CAR T cells by flow cytometry or RNA-seq, tumors were excised and digested postmortem using a cocktail of 1 mg/mL collagenase type IV (Sigma-Aldrich) and 0.02 mg/mL DNase (Sigma-Aldrich). After a 30-min digestion at 37°C, cells were passed through a 70-μm filter twice. Cells were then analyzed for various functional parameters, including cytokine production by flow cytometry directly *ex vivo*. In some experiments, isolated cells were restimulated with PMA (5 ng/mL) and ionomycin (1 μg/mL; Sigma-Aldrich) in the presence of GolgiPlug and GolgiStop (BD Biosciences) for 3 h before flow cytometry analysis.

RNA-Seq Analysis

Total RNA was isolated using an RNeasy kit (QIAGEN), as per the manufacturer's instructions, and RNA-seq libraries were prepared from ~400 ng of total RNA using the QuantSeq 3′ mRNA-Seq Library Prep Kit for Illumina (Lexogen), as per the manufacturer's instructions. Single-end, 75 bp RNA-seq short reads were generated using NextSeq (Illumina, San Diego, CA, USA). CASAVA 1.8.2 was used for base calling. Quality of the data was assessed using RNA-SeQC v.1.1.7.[39] To analyze differential gene expression, the data were quality trimmed using Cutadapt v.1.6 to remove random primer bias, and 3′ end trimming was performed to remove poly(A) tail-derived reads and alignment performed using HISAT2 against the mouse reference genome mm10. The subread software package 1.6.4 was used to count the number of reads per gene using gene definitions from Ensembl Release 96.[40] Gene counts were normalized using the TMM (trimmed means of M-values) method and converted into log2 counts per million (CPM) using edgeR v.3.8.5.[41,42] PCA was performed on normalized counts, and edgeR was applied for differential expression analysis between defined groups. All differentially expressed genes were filtered for false discovery rate (FDR) cutoff of 5% and fold-change cutoff >1. Volcano plots were used to represent differential gene expression between groups. Heatmaps for selected gene sets

were generated using the pheatmap R package, using row mean-centered and scaled gene-expression levels of log2(CPM + 0.5). Rows were grouped by hierarchical clustering using Euclidean distance and average linkage. Each group was sequenced in biological duplicates, and mean of CPM values was used.

For GSEA, all differentially expressed mouse genes between respective IL-7/IL-15 against IL-2/IL-7 CAR T cell groups were ranked according to fold change and compared to gene signatures for *Tcf7*$^{GFP+}$ versus *Tcf7*$^{GFP-}$ tumor-infiltrating CD8$^+$ T lymphocytes .[20] Likewise, differentially expressed genes for IL-7/IL-15 and IL-2/IL-7 human CAR T cells were compared to T cell gene signatures identified through unbiased clustering of CD45$^+$ cells from patient melanoma biopsies.[19] A gene signature for IL-7/IL-15 was generated using differentially expressed genes significantly modulated by IL-7/IL-15 compared to IL-2/IL-7 in both CD45RA and CD45RO human CAR T cells. The GSEA v.3.0 software (https://www.gsea-msigdb.org/gsea/index.jsp) was used to perform the analysis.[43] For analysis of murine CAR T cells *ex vivo*, the Enrichr database[44] was used using an FDR cutoff of 5% to screen 153 libraries unbiasedly. Several pathways from the GO biological process 2018 database[45] were identified, including T cell activation (GO: 0042110) and T cell differentiation (GO: 0030217).

Assay for Transposase-Accessible Chromatin Using Sequencing (ATAC-Seq) Analysis

ATAC-seq was performed using a protocol developed to reduce mitochondria from the transposition reaction.[46] Briefly, CAR T cells were cultured in IL-2/IL-7 or IL-7/IL-15, and on day 7 post-activation, duplicate samples were processed. Cells were washed once in ice-cold PBS and lysed in ATAC lysis buffer (0.1% Tween 20, 0.1% NP-40, 10 mM NaCl, 3 mM $MgCl_2$, 10 mM Tris HCl, pH 7.4). Tagmentation was performed with Tn5 transposase and 2× tagmentation DNA (TD) buffer (Nextera DNA Library Prep Kit; Illumina) at 37°C for 30 min. MinElute columns (QIAGEN; 28004) were used to purify TD, which was then amplified for 12 cycles using 2× KAPA HiFi HotStart ReadyMix (Kapa Biosystems; KK2602). Amplified libraries were then purified using MinElute columns (QIAGEN) and sequenced on an Illumina NextSeq 500 with 75 bp single-end reads. Library quality control (QC) and quantification were performed using D1000 high-sensitivity screen tape with a 4200 TapeStation Instrument (Agilent Technologies) with size selection of 200–500 bp using a Pippin Prep system (Sage Science). To analyze differential peaks, Fastq files generated were trimmed 15 bp on the 5′ end to remove random priming bias using Cutadapt (v.2.1), and 3′ end trimming was performed to remove Nextera transposase adaptor sequences introduced as a result of library preparation. Quality-trimmed reads were aligned to the mm10/GRCm38 genome using bowtie2 (v.2.3.4.1) with default settings.[47] SAMtools; v.1.9) was used for SAM to BAM file conversions, after which featureCounts, as part of the subread software package (v.1.5.2), was used to count reads within ATAC peaks identified using MACS (v.2.1.1) with settings–nomodel–extsize 300 and that were overlapping across samples, as determined by the merge function of (v.2.27.1).[48,49] Overlapping ATAC peaks were annotated to genes using HOMER (v.4.8).[50] With the use of voom, peak counts were normalized based on calculated normalization factors into log2 CPM and fitted to a linear model using limma.[51] Empirical Bayes smoothing of standard errors were used to calculate weights for each peak to determine differentially expressed peaks. PCA was performed on the top 5,000 variably expressed peaks using normalized peak counts. All differentially expressed peaks were filtered for adjusted p value (adj.p.value) cutoff of 5% and distance from transcriptional start site (TSS) of +10,000 bp (upstream) and −5,000 bp (downstream). MA plots were used to represent differential peak expression between groups. Heatmaps for selected peaks were generated using the pheatmap R package, using row mean-centered and scaled peak-expression levels of log2(CPM + 0.5). Rows were grouped by hierarchical clustering using Euclidean distance and average linkage. Each group was sequenced in biological duplicates, and mean of CPM values was used. Browser viewable TDF files were generated using igvtools (v.2.3.95) and resulting tracks were visualized using Integrative Genomics View (IGV; v.2.5.2).[52,53]

Statistics

Statistical tests were performed as indicated in the figure legends. A p value of less than 0.05 was considered significant.

SUPPLEMENTAL INFORMATION

Supplemental Information can be found online at https://doi.org/10.1016/j.ymthe.2020.07.018.

AUTHOR CONTRIBUTIONS

Conceptualization, L.G., P.K.D., and P.A.B.; Software, K.S., I.T., E.G., and S.J.V.; Formal Analysis, K.S., I.T., S.J.V., and L.M.K.; Investigation, L.G., K.S., M.A.H., I.G.H., J.L., A.X.Y.C., K.L.T., E.V.P., S.M., M.J.K., S.J.V., P.K.D., and P.A.B.; Resources, P.K.D. and P.A.B.; Writing – Original Draft, L.G., P.K.D., and P.A.B.; Writing – Review & Editing, L.G., K.S., I.G.H., J.L., P.K.D., and P.A.B.; Visualization, L.G. and P.A.B.; Supervision, B.J.S., R.W.J., I.A.P., P.J.N., L.M.K., P.K.D., and P.A.B.; Funding Acquisition, P.K.D. and P.A.B.

CONFLICTS OF INTEREST

The authors declare no competing interests.

ACKNOWLEDGMENTS

The authors would like to acknowledge the assistance from the staff of the Animal Facility, Flow Cytometry Facility, and Molecular Genomics Core at the Peter MacCallum Cancer Centre. This study was funded by the National Health and Medical Research Council (NHMRC; grant numbers 1132373 and 1122444). P.A.B. is supported by a National Breast Cancer Foundation Fellowship (ID number ECF-17-005). P.K.D. is supported by an NHMRC Senior Research Fellowship (APP1136680).

REFERENCES

1. Carpenito, C., Milone, M.C., Hassan, R., Simonet, J.C., Lakhal, M., Suhoski, M.M., Varela-Rohena, A., Haines, K.M., Heitjan, D.F., Albelda, S.M., et al. (2009). Control of large, established tumor xenografts with genetically retargeted human

T cells containing CD28 and CD137 domains. Proc. Natl. Acad. Sci. USA *106*, 3360–3365.

2. Finney, H.M., Lawson, A.D., Bebbington, C.R., and Weir, A.N. (1998). Chimeric receptors providing both primary and costimulatory signaling in T cells from a single gene product. J. Immunol. *161*, 2791–2797.
3. Zhong, X.S., Matsushita, M., Plotkin, J., Riviere, I., and Sadelain, M. (2010). Chimeric antigen receptors combining 4-1BB and CD28 signaling domains augment PI3kinase/AKT/Bcl-XL activation and CD8+ T cell-mediated tumor eradication. Mol. Ther. *18*, 413–420.
4. Tammana, S., Huang, X., Wong, M., Milone, M.C., Ma, L., Levine, B.L., June, C.H., Wagner, J.E., Blazar, B.R., and Zhou, X. (2010). 4-1BB and CD28 signaling plays a synergistic role in redirecting umbilical cord blood T cells against B-cell malignancies. Hum. Gene Ther. *21*, 75–86.
5. Mardiana, S., Solomon, B.J., Darcy, P.K., and Beavis, P.A. (2019). Supercharging adoptive T cell therapy to overcome solid tumor-induced immunosuppression. Sci. Transl. Med. *11*, eaaw2293.
6. Mardiana, S., Lai, J., House, I.G., Beavis, P.A., and Darcy, P.K. (2019). Switching on the green light for chimeric antigen receptor T-cell therapy. Clin. Transl. Immunology *8*, e1046.
7. Gattinoni, L., Klebanoff, C.A., and Restifo, N.P. (2012). Paths to stemness: building the ultimate antitumour T cell. Nat. Rev. Cancer *12*, 671–684.
8. Klebanoff, C.A., Gattinoni, L., and Restifo, N.P. (2012). Sorting through subsets: which T-cell populations mediate highly effective adoptive immunotherapy? J. Immunother. *35*, 651–660.
9. Hinrichs, C.S., Spolski, R., Paulos, C.M., Gattinoni, L., Kerstann, K.W., Palmer, D.C., Klebanoff, C.A., Rosenberg, S.A., Leonard, W.J., and Restifo, N.P. (2008). IL-2 and IL-21 confer opposing differentiation programs to CD8+ T cells for adoptive immunotherapy. Blood *111*, 5326–5333.
10. Klebanoff, C.A., Finkelstein, S.E., Surman, D.R., Lichtman, M.K., Gattinoni, L., Theoret, M.R., Grewal, N., Spiess, P.J., Antony, P.A., Palmer, D.C., et al. (2004). IL-15 enhances the in vivo antitumor activity of tumor-reactive CD8+ T cells. Proc. Natl. Acad. Sci. USA *101*, 1969–1974.
11. Kagoya, Y., Nakatsugawa, M., Yamashita, Y., Ochi, T., Guo, T., Anczurowski, M., Saso, K., Butler, M.O., Arrowsmith, C.H., and Hirano, N. (2016). BET bromodomain inhibition enhances T cell persistence and function in adoptive immunotherapy models. J. Clin. Invest. *126*, 3479–3494.
12. Fraietta, J.A., Nobles, C.L., Sammons, M.A., Lundh, S., Carty, S.A., Reich, T.J., Cogdill, A.P., Morrissette, J.J.D., DeNizio, J.E., Reddy, S., et al. (2018). Disruption of TET2 promotes the therapeutic efficacy of CD19-targeted T cells. Nature *558*, 307–312.
13. Leone, R.D., Sun, I.M., Oh, M.H., Sun, I.H., Wen, J., Englert, J., and Powell, J.D. (2018). Inhibition of the adenosine A2a receptor modulates expression of T cell coinhibitory receptors and improves effector function for enhanced checkpoint blockade and ACT in murine cancer models. Cancer Immunol. Immunother. *67*, 1271–1284.
14. John, L.B., Devaud, C., Duong, C.P., Yong, C.S., Beavis, P.A., Haynes, N.M., Chow, M.T., Smyth, M.J., Kershaw, M.H., and Darcy, P.K. (2013). Anti-PD-1 antibody therapy potently enhances the eradication of established tumors by gene-modified T cells. Clin. Cancer Res. *19*, 5636–5646.
15. Rupp, L.J., Schumann, K., Roybal, K.T., Gate, R.E., Ye, C.J., Lim, W.A., and Marson, A. (2017). CRISPR/Cas9-mediated PD-1 disruption enhances anti-tumor efficacy of human chimeric antigen receptor T cells. Sci. Rep. *7*, 737.
16. Beavis, P.A., Henderson, M.A., Giuffrida, L., Mills, J.K., Sek, K., Cross, R.S., Davenport, A.J., John, L.B., Mardiana, S., Slaney, C.Y., et al. (2017). Targeting the adenosine 2A receptor enhances chimeric antigen receptor T cell efficacy. J. Clin. Invest. *127*, 929–941.
17. Chong, E.A., Melenhorst, J.J., Lacey, S.F., Ambrose, D.E., Gonzalez, V., Levine, B.L., June, C.H., and Schuster, S.J. (2017). PD-1 blockade modulates chimeric antigen receptor (CAR)-modified T cells: refueling the CAR. Blood *129*, 1039–1041.
18. Heczey, A., Louis, C.U., Savoldo, B., Dakhova, O., Durett, A., Grilley, B., Liu, H., Wu, M.F., Mei, Z., Gee, A., et al. (2017). CAR T Cells Administered in Combination with Lymphodepletion and PD-1 Inhibition to Patients with Neuroblastoma. Mol. Ther. *25*, 2214–2224.
19. Sade-Feldman, M., Yizhak, K., Bjorgaard, S.L., Ray, J.P., de Boer, C.G., Jenkins, R.W., Lieb, D.J., Chen, J.H., Frederick, D.T., Barzily-Rokni, M., et al. (2019). Defining T Cell States Associated with Response to Checkpoint Immunotherapy in Melanoma. Cell *176*, 404.
20. Siddiqui, I., Schaeuble, K., Chennupati, V., Fuertes Marraco, S.A., Calderon-Copete, S., Pais Ferreira, D., Carmona, S.J., Scarpellino, L., Gfeller, D., Pradervand, S., et al. (2019). Intratumoral Tcf1(+)PD-1(+)CD8(+) T Cells with Stem-like Properties Promote Tumor Control in Response to Vaccination and Checkpoint Blockade Immunotherapy. Immunity *50*, 195–211.e10.
21. Gattinoni, L., Zhong, X.S., Palmer, D.C., Ji, Y., Hinrichs, C.S., Yu, Z., Wrzesinski, C., Boni, A., Cassard, L., Garvin, L.M., et al. (2009). Wnt signaling arrests effector T cell differentiation and generates CD8+ memory stem cells. Nat. Med. *15*, 808–813.
22. Mardiana, S., John, L.B., Henderson, M.A., Slaney, C.Y., von Scheidt, B., Giuffrida, L., Davenport, A.J., Trapani, J.A., Neeson, P.J., Loi, S., et al. (2017). A Multifunctional Role for Adjuvant Anti-4-1BB Therapy in Augmenting Antitumor Response by Chimeric Antigen Receptor T Cells. Cancer Res. *77*, 1296–1309.
23. Miller, B.C., Sen, D.R., Al Abosy, R., Bi, K., Virkud, Y.V., LaFleur, M.W., Yates, K.B., Lako, A., Felt, K., Naik, G.S., et al. (2019). Subsets of exhausted $CD8^+$ T cells differentially mediate tumor control and respond to checkpoint blockade. Nat. Immunol. *20*, 326–336.
24. Man, K., Gabriel, S.S., Liao, Y., Gloury, R., Preston, S., Henstridge, D.C., Pellegrini, M., Zehn, D., Berberich-Siebelt, F., Febbraio, M.A., et al. (2017). Transcription Factor IRF4 Promotes CD8(+) T Cell Exhaustion and Limits the Development of Memory-like T Cells during Chronic Infection. Immunity *47*, 1129–1141.e5.
25. Michie, J., Beavis, P.A., Freeman, A.J., Vervoort, S.J., Ramsbottom, K.M., Narasimhan, V., Lelliott, E.J., Lalaoui, N., Ramsay, R.G., Johnstone, R.W., et al. (2019). Antagonism of IAPs Enhances CAR T-cell Efficacy. Cancer Immunol. Res. *7*, 183–192.
26. Jadhav, R.R., Im, S.J., Hu, B., Hashimoto, M., Li, P., Lin, J.X., Leonard, W.J., Greenleaf, W.J., Ahmed, R., and Goronzy, J.J. (2019). Epigenetic signature of PD-1+ TCF1+ CD8 T cells that act as resource cells during chronic viral infection and respond to PD-1 blockade. Proc. Natl. Acad. Sci. USA *116*, 14113–14118.
27. Kurtulus, S., Madi, A., Escobar, G., Klapholz, M., Nyman, J., Christian, E., Pawlak, M., Dionne, D., Xia, J., Rozenblatt-Rosen, O., et al. (2019). Checkpoint Blockade Immunotherapy Induces Dynamic Changes in PD-1(-)CD8(+) Tumor-Infiltrating T Cells. Immunity *50*, 181–194.e6.
28. Fraietta, J.A., Lacey, S.F., Orlando, E.J., Pruteanu-Malinici, I., Gohil, M., Lundh, S., Boesteanu, A.C., Wang, Y., O'Connor, R.S., Hwang, W.T., et al. (2018). Determinants of response and resistance to CD19 chimeric antigen receptor (CAR) T cell therapy of chronic lymphocytic leukemia. Nat. Med. *24*, 563–571.
29. Zeng, R., Spolski, R., Finkelstein, S.E., Oh, S., Kovanen, P.E., Hinrichs, C.S., Pise-Masison, C.A., Radonovich, M.F., Brady, J.N., Restifo, N.P., et al. (2005). Synergy of IL-21 and IL-15 in regulating CD8+ T cell expansion and function. J. Exp. Med. *201*, 139–148.
30. Xu, Y., Zhang, M., Ramos, C.A., Durett, A., Liu, E., Dakhova, O., Liu, H., Creighton, C.J., Gee, A.P., Heslop, H.E., et al. (2014). Closely related T-memory stem cells correlate with in vivo expansion of CAR.CD19-T cells and are preserved by IL-7 and IL-15. Blood *123*, 3750–3759.
31. Alizadeh, D., Wong, R.A., Yang, X., Wang, D., Pecoraro, J.R., Kuo, C.F., Aguilar, B., Qi, Y., Ann, D.K., Starr, R., et al. (2019). IL15 Enhances CAR-T Cell Antitumor Activity by Reducing mTORC1 Activity and Preserving Their Stem Cell Memory Phenotype. Cancer Immunol. Res. *7*, 759–772.
32. Crompton, J.G., Sukumar, M., Roychoudhuri, R., Clever, D., Gros, A., Eil, R.L., Tran, E., Hanada, K., Yu, Z., Palmer, D.C., et al. (2015). Akt inhibition enhances expansion of potent tumor-specific lymphocytes with memory cell characteristics. Cancer Res. *75*, 296–305.
33. Tyrakis, P.A., Palazon, A., Macias, D., Lee, K.L., Phan, A.T., Veliça, P., You, J., Chia, G.S., Sim, J., Doedens, A., et al. (2016). S-2-hydroxyglutarate regulates $CD8^+$ T-lymphocyte fate. Nature *540*, 236–241.
34. Sabatino, M., Hu, J., Sommariva, M., Gautam, S., Fellowes, V., Hocker, J.D., Dougherty, S., Qin, H., Klebanoff, C.A., Fry, T.J., et al. (2016). Generation of clinical-grade CD19-specific CAR-modified CD8+ memory stem cells for the treatment of human B-cell malignancies. Blood *128*, 519–528.

35. Odorizzi, P.M., Pauken, K.E., Paley, M.A., Sharpe, A., and Wherry, E.J. (2015). Genetic absence of PD-1 promotes accumulation of terminally differentiated exhausted CD8+ T cells. J. Exp. Med. *212*, 1125–1137.

36. Kershaw, M.H., Jackson, J.T., Haynes, N.M., Teng, M.W., Moeller, M., Hayakawa, Y., Street, S.E., Cameron, R., Tanner, J.E., Trapani, J.A., et al. (2004). Gene-engineered T cells as a superior adjuvant therapy for metastatic cancer. J. Immunol. *173*, 2143–2150.

37. Haynes, N.M., Snook, M.B., Trapani, J.A., Cerruti, L., Jane, S.M., Smyth, M.J., and Darcy, P.K. (2001). Redirecting mouse CTL against colon carcinoma: superior signaling efficacy of single-chain variable domain chimeras containing TCR-zeta vs Fc epsilon RI-gamma. J. Immunol. *166*, 182–187.

38. Westwood, J.A., Smyth, M.J., Teng, M.W., Moeller, M., Trapani, J.A., Scott, A.M., Smyth, F.E., Cartwright, G.A., Power, B.E., Hönemann, D., et al. (2005). Adoptive transfer of T cells modified with a humanized chimeric receptor gene inhibits growth of Lewis-Y-expressing tumors in mice. Proc. Natl. Acad. Sci. USA *102*, 19051–19056.

39. DeLuca, D.S., Levin, J.Z., Sivachenko, A., Fennell, T., Nazaire, M.D., Williams, C., Reich, M., Winckler, W., and Getz, G. (2012). RNA-SeQC: RNA-seq metrics for quality control and process optimization. Bioinformatics *28*, 1530–1532.

40. Zerbino, D.R., Achuthan, P., Akanni, W., Amode, M.R., Barrell, D., Bhai, J., Billis, K., Cummins, C., Gall, A., Girón, C.G., et al. (2018). Ensembl 2018. Nucleic Acids Res. *46*, D754–D761.

41. Robinson, M.D., McCarthy, D.J., and Smyth, G.K. (2010). edgeR: a Bioconductor package for differential expression analysis of digital gene expression data. Bioinformatics *26*, 139–140.

42. McCarthy, D.J., Chen, Y., and Smyth, G.K. (2012). Differential expression analysis of multifactor RNA-Seq experiments with respect to biological variation. Nucleic Acids Res. *40*, 4288–4297.

43. Subramanian, A., Tamayo, P., Mootha, V.K., Mukherjee, S., Ebert, B.L., Gillette, M.A., Paulovich, A., Pomeroy, S.L., Golub, T.R., Lander, E.S., and Mesirov, J.P. (2005). Gene set enrichment analysis: a knowledge-based approach for interpreting genome-wide expression profiles. Proc. Natl. Acad. Sci. USA *102*, 15545–15550.

44. Kuleshov, M.V., Jones, M.R., Rouillard, A.D., Fernandez, N.F., Duan, Q., Wang, Z., Koplev, S., Jenkins, S.L., Jagodnik, K.M., Lachmann, A., et al. (2016). Enrichr: a comprehensive gene set enrichment analysis web server 2016 update. Nucleic Acids Res. *44* (W1), W90–W97.

45. Ashburner, M., Ball, C.A., Blake, J.A., Botstein, D., Butler, H., Cherry, J.M., Davis, A.P., Dolinski, K., Dwight, S.S., Eppig, J.T., et al.; The Gene Ontology Consortium (2000). Gene ontology: tool for the unification of biology. Nat. Genet. *25*, 25–29.

46. Corces, M.R., Trevino, A.E., Hamilton, E.G., Greenside, P.G., Sinnott-Armstrong, N.A., Vesuna, S., Satpathy, A.T., Rubin, A.J., Montine, K.S., Wu, B., et al. (2017). An improved ATAC-seq protocol reduces background and enables interrogation of frozen tissues. Nat. Methods *14*, 959–962.

47. Langmead, B., Trapnell, C., Pop, M., and Salzberg, S.L. (2009). Ultrafast and memory-efficient alignment of short DNA sequences to the human genome. Genome Biol. *10*, R25.

48. Zhang, Y., Liu, T., Meyer, C.A., Eeckhoute, J., Johnson, D.S., Bernstein, B.E., Nusbaum, C., Myers, R.M., Brown, M., Li, W., and Liu, X.S. (2008). Model-based analysis of ChIP-Seq (MACS). Genome Biol. *9*, R137.

49. Quinlan, A.R., and Hall, I.M. (2010). BEDTools: a flexible suite of utilities for comparing genomic features. Bioinformatics *26*, 841–842.

50. Heinz, S., Benner, C., Spann, N., Bertolino, E., Lin, Y.C., Laslo, P., Cheng, J.X., Murre, C., Singh, H., and Glass, C.K. (2010). Simple combinations of lineage-determining transcription factors prime cis-regulatory elements required for macrophage and B cell identities. Mol. Cell *38*, 576–589.

51. Ritchie, M.E., Phipson, B., Wu, D., Hu, Y., Law, C.W., Shi, W., and Smyth, G.K. (2015). limma powers differential expression analyses for RNA-sequencing and microarray studies. Nucleic Acids Res. *43*, e47.

52. Robinson, J.T., Thorvaldsdóttir, H., Winckler, W., Guttman, M., Lander, E.S., Getz, G., and Mesirov, J.P. (2011). Integrative genomics viewer. Nat. Biotechnol. *29*, 24–26.

53. Thorvaldsdóttir, H., Robinson, J.T., and Mesirov, J.P. (2013). Integrative Genomics Viewer (IGV): high-performance genomics data visualization and exploration. Brief. Bioinform. *14*, 178–192.